ACS APPLIED MATERIALS & INTERFACES

Research Article

www.acsami.org

Electrospun Composite Nanofiber Yarns Containing Oriented Graphene Nanoribbons

Hidetoshi Matsumoto,*[,†] Shinji Imaizumi,[†] Yuichi Konosu,[†] Minoru Ashizawa,[†] Mie Minagawa,[†] Akihiko Tanioka,*[,†] Wei Lu,[‡] and James M. Tour[‡]

[†]Department of Organic and Polymeric Materials, Tokyo Institute of Technology, Mail Box S8-27, 2-12-1 Ookayama, Meguro-ku, Tokyo 152-8552, Japan

[‡]Departments of Chemistry and Mechanical Engineering and Materials Science and the Smalley Institute for Nanoscale Science and Technology, Rice University, MS222, 6100 Main Street, Houston, Texas 77005, United States

Supporting Information

ABSTRACT: The graphene nanoribbon (GNR)/carbon composite nanofiber yarns were prepared by electrospinning from poly(acrylonitrile) (PAN) containing graphene oxide nanoribbons (GONRs), and successive twisting and carbonization. The electrospinning process can exert directional shear force coupling with the external electric field to the flow of the spinning solution. During electrospinning, the well-dispersed GONRs were highly oriented along the fiber axis in an electrified thin liquid jet. The addition of GONRs at a low weight fraction significantly improved the mechanical properties of the composite nanofiber yarns. In addition, the carbonization of the matrix polymer enhanced not only the mechanical but also the electrical properties of the composites. The electrical conductivity of the carbonized composite yarns containing 0.5 wt % GONR showed the maximum value of 165 S cm^{-1}. It is larger than the maximum value of the reported electrospun carbon composite yarns. Interestingly, it is higher than the conductivities of both the PAN-based pristine CNF yarns (77 S cm^{-1}) and the monolayer GNRs (54 S cm^{-1}). These results and Raman spectroscopy supported the hypothesis that the oriented GONRs contained in the PAN nanofibers effectively functioned as not only the 1-D nanofiller but also the nanoplatelet promoter of stabilization and template agent for the carbonization.

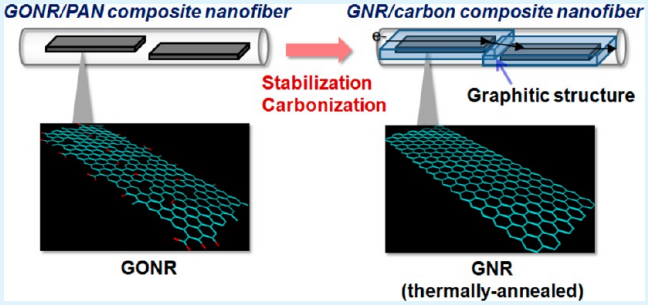

KEYWORDS: *graphene nanoribbon, nanocomposite, nanofiber, electrospinning, mechanical properties, electrical properties*

INTRODUCTION

Graphene, a single-atom-thick sheet of sp^2-bonded carbon atoms, has recently received considerable interest due to its unique features, such as extraordinary electronic properties,[1] mechanical strength,[2] and ultrahigh thermal conductivity.[3] Graphene nanoribbons (GNRs), thin elongated strips of graphene with a high length-to-width ratio and straight edges, are a new class of pseudo-one-dimensional (1-D) nanocarbons. They have also attracted attention because of their novel electronic and spin transport properties.[4−7] GNRs have been produced by a variety of methods from chemical vapor deposition (CVD), through chemical treatments of graphite to the unzipping of CNTs.[8] Tour et al. reported a high-yielding procedure for the production of large amounts of graphene oxide nanoribbons (GONRs) through the oxidative longitudinal unzipping of multiwalled carbon nanotubes (MWNTs) in a sulfuric acid (H_2SO_4) solution of potassium permanganate ($KMnO_4$).[4] The GONRs can be used in this oxidized and exfoliated form and then reduced to the more conductive GNRs using chemical or thermal methods. The large quantities that can be made using this technique could provide enough material for composites, fibers, large-scale electronics, and other applications.

Recently, some researchers have reported that the addition of a low fraction of GNRs (less than 0.5 wt %) resulted in a significant improvement in the mechanical strength and electrical properties of the composites.[9,10] GNRs should provide good integration with a polymer matrix due to its highly crystalline planar structure, which provides a large interfacial area for $\pi-\pi$ stacking with the polymer matrix.[8] In addition, the carboxylic and hydroxyl functional groups on the basal planes and edges of the starting GONR can act as linkers between the GONR and polymer and provide mechanical strength.[11] This paper focuses on the preparation of GONR/polymer and GNR/carbon composite nanofiber yarns, prepared by electrospinning. Electrospinning is a simple and versatile method for the formation of continuous thin fibers ranging from several nanometers to tens of micrometers,[12,13] which is based on an electrohydrodynamic phenomenon.[14] Therefore,

Received: April 3, 2013
Accepted: June 13, 2013
Published: June 13, 2013

   dx.doi.org/10.1021/am401161b | ACS Appl. Mater. Interfaces 2013, 5, 6225−6231

the electrospinning process can exert directional shear force coupling with the external electric field to the flow of the spinning solution.[15] Our previous study showed that the 1-D nanomaterial, MWNTs, were highly oriented along the fiber axis during electrospinning and the filling of the oriented 1-D nanofillers in the composites significantly improved their mechanical and electrical properties.[16] We now expect that a pseudo-1-D nanomaterial, GONRs, can be also highly oriented in the electrospun thin fibers and the filling of the oriented GONRs in the composites improves their properties.

In this study, we synthesized GONRs with high length-to-width ratios (average length: 3 μm; average width: 140 nm) through the nanotube unzipping process by chemical oxidation. We used the obtained GONRs and poly(acrylonitrile) as the 1-D nanomaterial filler and polymer matrix, respectively. We first produced GONR/poly(acrylonitrile) (PAN) composite nanofiber yarns containing oriented GONRs by electrospinning and twisting. In addition, we stabilized and carbonized composites to provide GNR/carbon nanofiber yarns. The aims of this study are (i) to prepare novel nanocarbon composite nanofibers, GONR/polymer and GNR/carbon composite nanofiber yarns, and (ii) to investigate the additive effects of GONRs on the mechanical and electrical properties of the prepared composite nanofiber yarns.

EXPRIMENTAL SECTION

Materials. As precursors of the GONRs, multiwalled carbon nanotubes (MWNT-7, average diameter = 50 nm, aspect ratio > 100, lot number: 071223) were obtained from Hodogaya Chemical, Japan. Sulfuric acid (H_2SO_4), phosphoric acid (H_3PO_4), and potassium permanganate ($KMnO_4$) of extra-pure grade were purchased from Wako, Japan. Poly(acrylonitrile) (PAN) with a molecular weight of 150 000 was purchased from Sigma-Aldrich, USA. *N*,*N*-dimethylformamide (DMF) of extra-pure grade was obtained from Wako, Japan. These reagents were used without further purification.

Preparation of Graphene Oxide Nanoribbons. The GONRs were prepared by the oxidation and longitudinal unzipping of the MWNTs, as previously described.[17] MWNTs (1.00 g) were dispersed in 180 mL of H_2SO_4 with stirring for 1 h. H_3PO_4 (85%, 20 mL) was then added to the dispersion, and the mixture was stirred for another 15 min before the addition of $KMnO_4$ (6 g, 1 g/portion, finished in 30 min). The reaction mixture was heated at 55 °C for 1 h, and then cooled to room temperature. Thereafter, the reaction mixture was poured into 500 mL of ice containing H_2O_2 (30 wt %, 10 mL). The product was filtered over a poly(tetrafluoroethylene) (PTFE) membrane (450 nm pore size). The brown filter cake was washed two times with 10 wt % HCl (2 × 200 mL), acetone (2 × 100 mL), and ether (2 × 100 mL). The removal of the solvent under vacuum condition (at 60 °C, 24 h) gave a product (1.85 g).

Electrospinning. For preparation of the spinning solution, DMF was used as the solvent of PAN and GONR. GONR was added to the 8 wt % PAN/DMF solution with 0−10 wt % GONR fractions and then stirred at the speed of 1000 rpm for 1 day. The solute compositions in the spinning solutions are as follows: GONR/PAN = 0/100, 0.1/99.9, 0.3/99.7, 0.5/99.5, 0.7/99.3, 1/99, 2/98, 3/97, 5/95, and 10/90 in wt/wt. The electrospinning device was the same as that used in our previous study (Figure 1).[16] The polymer solution was contained in a syringe with a stainless steel nozzle (0.2 mm internal diameter). The nozzle was connected to a high-voltage regulated DC power supply (HAR-100P0.3, Matsusada Precision, Japan). A constant volume flow rate was maintained via a syringe-type infusion pump (MCIP-III, Minato Concept, Japan). A rotating disk (disk diameter: 250 mm; width: 10 mm) was used as a collector to align the electrospun fibers. The distance between the nozzle tip and the collector was 100 mm, the applied voltage was 30 kV, the flow rate was 5 μL/min, and the rotating speed of the collector was 1000 rpm. The duration of the spinning was 20 min. All spinnings were carried out at 25 ± 1 °C and at less than 35% relative humidity.

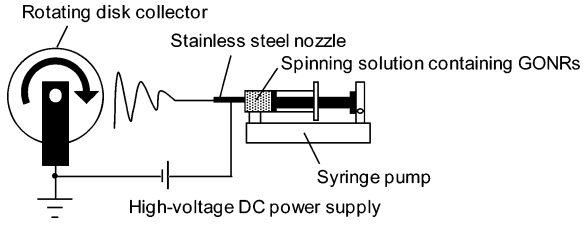

Figure 1. Schematic diagram of the apparatus used for electrospinning.

Preparation of Yarns. Yarns were fabricated by twisting of the electrospun aligned fibers. Thereafter, heat treatments were carried out with the yarns in tension at 120 °C for 2 h under a high vacuum condition in order to decrease the voids in the yarns. The diameter of the prepared twisted yarns was around 50 μm.

Characterization and Instruments. The morphologies of the prepared GONRs and composite nanofiber yarns were characterized using a field-emission scanning electron microscope (FE-SEM, SUPRA 40, Zeiss, Germany) and a scanning electron microscope (SEM, JCM-5700, JEOL, Japan) operated at 10 kV. The morphology and thickness of the GONRs were observed using an atomic force microscope (AFM, SPA400, SII Nanotechnology, Japan). The inner structure of the prepared composite nanofiber was observed using a transmission electron microscope (TEM, H-7650, Hitachi, Japan) operated at 100 kV. The Raman spectra were measured using a Raman microscopy system (NRS-2100, JASCO, Japan). As a light source, 514.5 nm radiation from an Ar-ion laser was used. The irradiated power of the excitation beam was about 10 mW at the sample surface. The spectra were obtained with a 100 s integration time. The X-ray photoelectron spectra (XPS) were measured by a scanning ESCA microprobe (Quantum-2000, ULVAC-PHI, Japan). The pyrolytic behaviors of the stabilized PAN and GONR/PAN composite nanofiber yarns in N_2 was characterized by a thermogravimetric-differential thermal analysis (TG-DTA, TG8120, Rigaku, Japan). The electrical conductivity of the prepared yarn was evaluated using the DC four-probe method by an impedance analyzer (model 1225B frequency response analyzer and model SI 1287 electrochemical interface, Solartron, U.K.). Five samples were measured for each yarn. The mechanical properties of the prepared yarns were tested by a universal testing machine (STA-1150, Orientec, Japan). The initial gauge length of the sample was 20 mm, and the strain rates were 1 and 0.05 mm min^{-1} for the as-spun yarns and carbonized yarns, respectively. Ten samples were measured for each yarn.

RESULTS AND DISCUSSION

Fabrication of GONR/PAN Composite Nanofibers. The GONRs used in this study were prepared by the unzipping of MWNTs in the presence of a second acid (H_3PO_4) besides the H_2SO_4/$KMnO_4$ mixture.[17] The typical field-emission scanning electron microscopy (FE-SEM) images show that the starting MWNT with a diameter of 55 nm and a length of 7 μm (Figure 2a) resulted in a nanoribbon with a width of 140 nm and a length of 2.8 μm (Figure 2b). The resulting GONRs have a shorter length, but still maintain a high aspect ratio with straight edges. The atomic force microscopy (AFM) image shows a single-layer GONR with the average thickness of 0.85 nm (Figure 2c), which is comparable to the *d* value of 0.82 nm observed by an X-ray diffraction (XRD) analysis (Figure S1a, Supporting Information) and agrees well with the theoretically calculated height for a single layer of GO bearing oxygen-containing functionalities on each side (0.75 nm).[18] The X-ray photoelectron spectroscopy (XPS) spectra (Figure S1b, Supporting Information) exhibited a clear oxidized carbon peak at 286.1 eV in the GONR. The Raman spectra and the

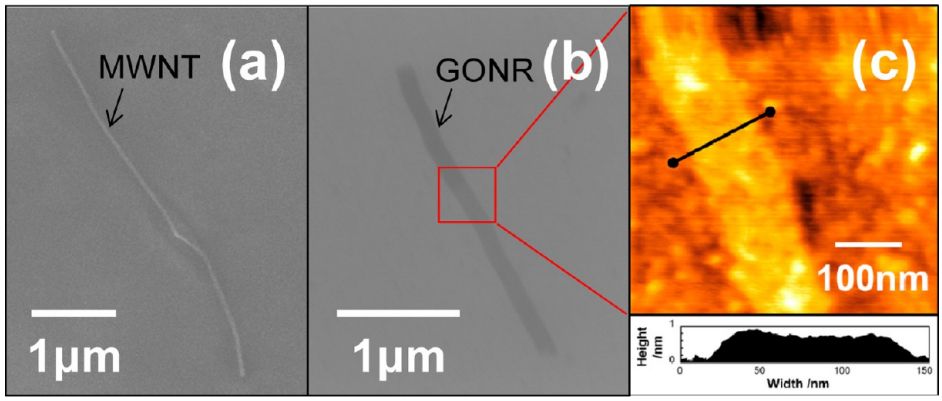

Figure 2. Typical surface SEM images of (a) the starting MWNT and (b) the prepared GONR. (c) AFM image of the GONR. All samples were deposited on a SiO_2 substrate.

mapping images are shown in Figure S2 (Supporting Information). These results clearly show that the MWNTs were successfully unzipped and then exfoliated to form the GONRs through chemical oxidation. The prepared GONRs were dispersed in PAN/DMF solutions of different concentrations and then used for electrospinning.

We succeeded in preparing aligned GONR/PAN composite nanofibers from the spinning solutions (GONR/PAN = 0/100, 0.1/99.9, 0.3/99.7, 0.5/99.5, 0.7/99.3, 1/99, 2/98, 3/97, 5/95, 10/90 in wt/wt) with a good spinnability. Figure 3 shows the aligned GONR/PAN composite nanofibers. For the fibers containing 0–2 wt % GONR, their diameters are around 200 nm and their morphologies were bead-free and smooth (Figure 3a–f). For the fibers containing 5 wt % GONR, on the other hand, we found some rough surface regions on the fiber (Figure 3g) due to the large agglomeration of the GONRs in the polymer matrix, as supported by the TEM observations (Figure 4). The yarns were prepared by twisting of the aligned nanofibers, and the diameter of the yarns was approximately 50 μm (Figure 3h).

To characterize the orientation of the GONRs in the composite fibers, a TEM analysis was performed. The TEM images of the composite fibers below 0.5 wt % GONR showed that the GONRs were highly oriented along the fiber axis of the fibers as expected (some parts formed a wavy structure). Typical TEM images of oriented ribbons in the composite fibers with 0.5 wt % GONR are shown in Figure 4a,b. The GONRs were oriented to the fiber axis by the electrified thin liquid jet during electrospinning. The electrospinning process can exert directional shear force coupling with the external electric field to the flow of the spinning solution. Our previous studies showed that 1-D nanomaterials (e.g., CNTs)[16] and rigid molecules (e.g., liquid crystalline polymers)[19,20] were highly oriented along the fiber axis of the electrospun nanofibers by the synergistic effect of the external electric field and shear force. At a greater than 0.7 wt % GONR fraction, on the other hand, the agglomerates of GONRs were formed (i.e., GONRs were not well-dispersed and not oriented) in the fibers. The number and size of the agglomerates increased with an increase in the weight fraction of GONR in the composite nanofibers. Typical agglomerates in the composite fibers with 5 wt % GONR are shown in Figure 4c,d.

The additive effects of the GONRs on the mechanical properties (i.e., elongation, strength, and Young's modulus) of the as-spun GONR/PAN composite nanofiber yarns were obtained from the stress–strain (S–S) curves (Figure S3, Supporting Information). These results are shown in Figure 5. The yarn's elongation decreased from 12% to 3% with an increase in the GONR content in the fiber. This indicated that the GONRs in the nanofiber hinder the movement of the polymer chains. The tensile strength and Young's modulus showed a peak for the 0.5 and 0.5–1 wt % GONR fractions, respectively. The maximum tensile strength of 179 MPa and the maximum Young's modulus of 5.5 GPa were 260% and 170% higher than the strength (69.7 MPa) and the modulus

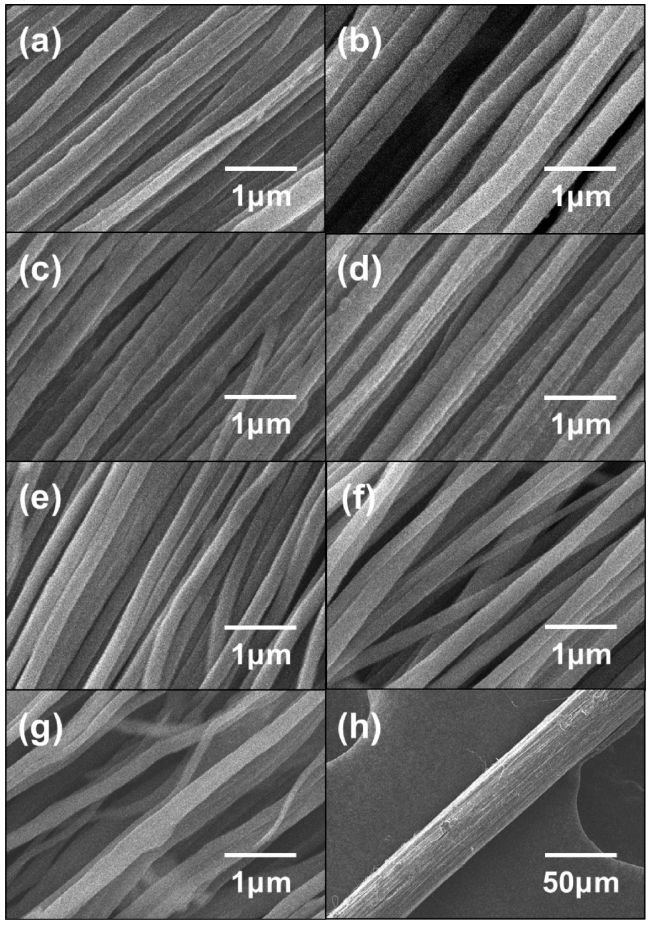

Figure 3. Surface SEM images of the GONR/PAN composite nanofibers. (a) Pristine PAN nanofibers. The composite nanofibers contain (b) 0.1, (c) 0.3, (d) 0.5, (e) 1, (f) 2, and (g) 5 wt % GONR, and (h) nanofiber yarn of (d).

dx.doi.org/10.1021/am401161b | ACS Appl. Mater. Interfaces 2013, 5, 6225–6231

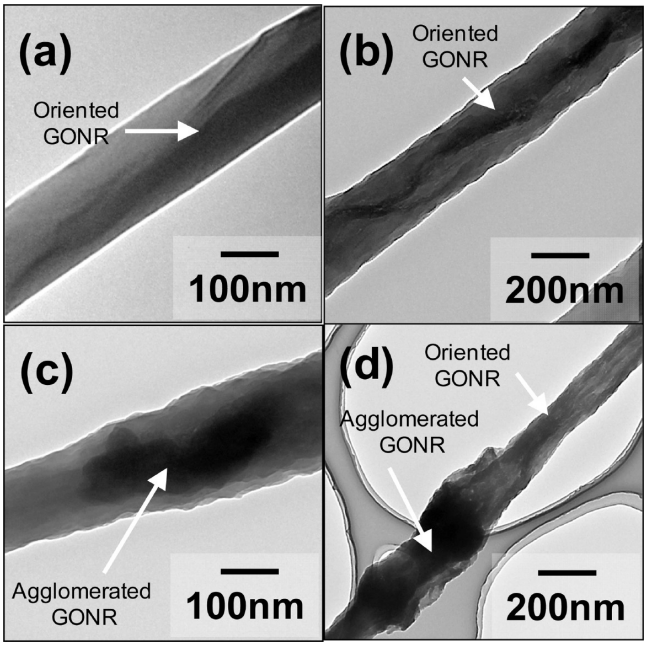

Figure 4. Typical TEM images of the as-spun GONR/PAN composite nanofiber. Composite nanofibers contain (a, b) 0.5 wt % and (c, d) 5 wt % GONR.

(3.34 GPa) of the pristine PAN nanofiber yarns, respectively. These values are also 220% and 180% higher than the reported value of the strength (80 MPa) and the modulus (3.1 GPa) for the functionalized-MWNT/PAN composite nanofibers (f-MWNT/PAN = 5/95 wt/wt), respectively.[21] This is due to that the higher specific surface area of the nanoribbon than that of the nanotube contributes to the better interfacial contact to the polymer matrix and the better additive effect of the nanoribbon on mechanical properties, as Tour and Koratkar et al. pointed out.[9] At a low GONR fraction, the highly oriented GONRs (Figure 4a,b) improved the interfacial contact and interaction between the GONR and polymer matrix. At a higher GONR fraction (>0.5 wt %), on the other hand, the GONRs would be poorly dispersed and easily form agglomerates with decreased interfacial contact between the GONR and polymer matrix (Figure 4c,d). This is responsible for the observation of the maximum tensile strength and Young's modulus.

Preparation of GNR/Carbon Composite Nanofiber Yarns. To carbonize the matrix of the composites, stabilization and carbonization treatments were carried out. The prepared GONR/PAN composite nanofiber yarns were heated at 230 °C for 3 h in the air for stabilizing, and then they were heated at 1000 °C for 1 h in a nitrogen atmosphere for carbonization. During the carbonization, the GONRs can be reduced in the nitrogen atmosphere. To characterize the stabilized GONR/PAN composite nanofiber yarns, Fourier transform infrared spectroscopy (FT-IR) and thermogravimetric-differential thermal analysis (TG-DTA) measurements were carried out (Figures S4 and S5, Supporting Information). Figure 6 shows the surface SEM images of the GNR/carbon composite nanofiber yarns. The morphology and shape of the nanofiber yarns were maintained after carbonization.

To elucidate the internal structure of the GNR/carbon composite nanofiber yarns, Raman spectroscopy measurements were performed. Figure 7a shows the Raman spectra of the

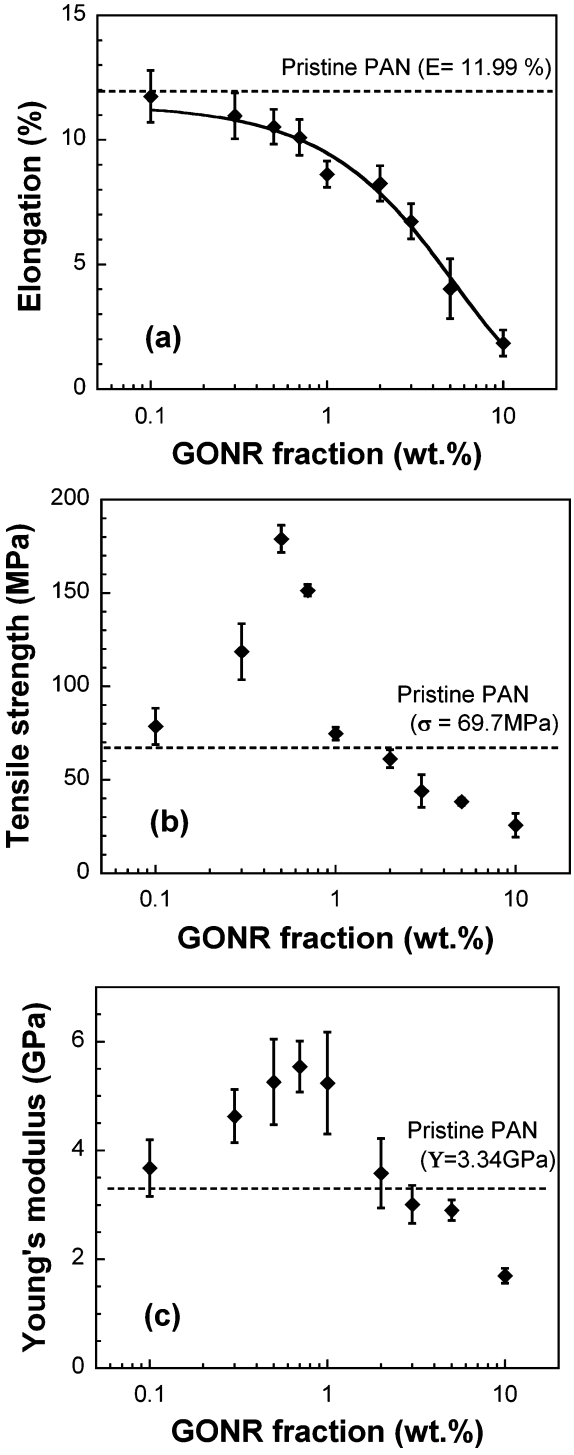

Figure 5. Additive effects of GONR on (a) elongation, (b) tensile strength, and (c) Young's modulus of the composite nanofiber yarns.

GNR/carbon composite nanofiber yarns. A D-band around 1360 cm^{-1} corresponds to the amorphous carbon and structural defects (A_{1g}, D breathing mode), and a G-band around 1580 cm^{-1} corresponds to the graphite structures and tangential shearing mode of the carbon atom (E_{2g}, G mode). The relative intensity ratio of the D-band to the G-band, I_D/I_G, which is called the "*R*-value", indicates the amount of structurally ordered graphite crystallites in the carbonaceous materials.[22,23] The I_D/I_G ratio for the carbonized yarns showed a peak at the 0.5 wt % GONR fraction (Figure 7b). At a greater

dx.doi.org/10.1021/am401161b | ACS Appl. Mater. Interfaces 2013, 5, 6225−6231

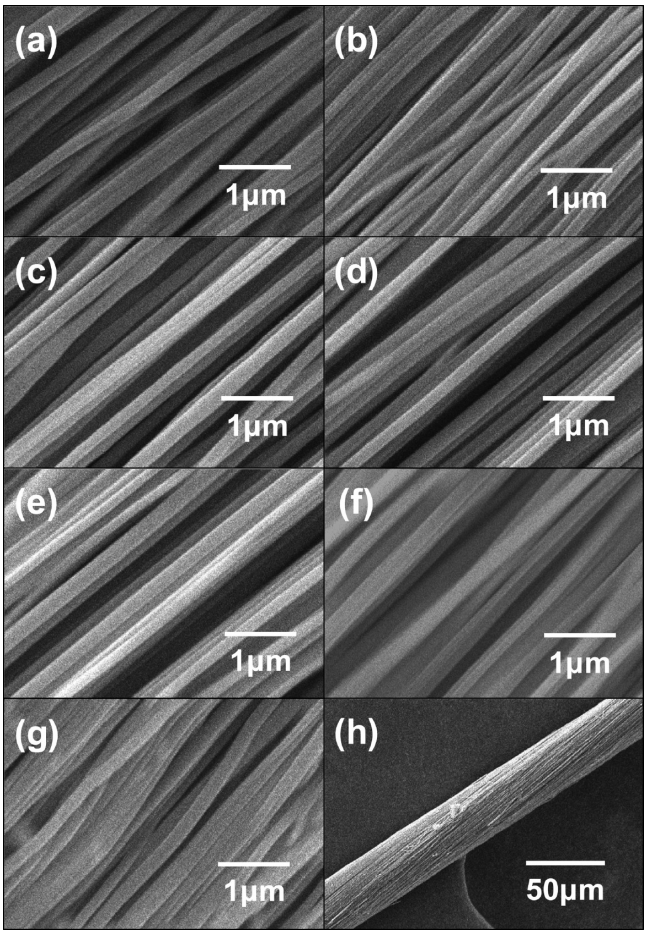

Figure 6. Surface SEM images of the GNR/carbon composite nanofiber yarns. (a) Pristine PAN-based carbon nanofiber yarn. Composite nanofiber yarns contain (b) 0.1, (c) 0.3, (d) 0.5, (e) 1, (f) 2, and (g) 5 wt % of the GONR, and (h) low-magnification image of (d).

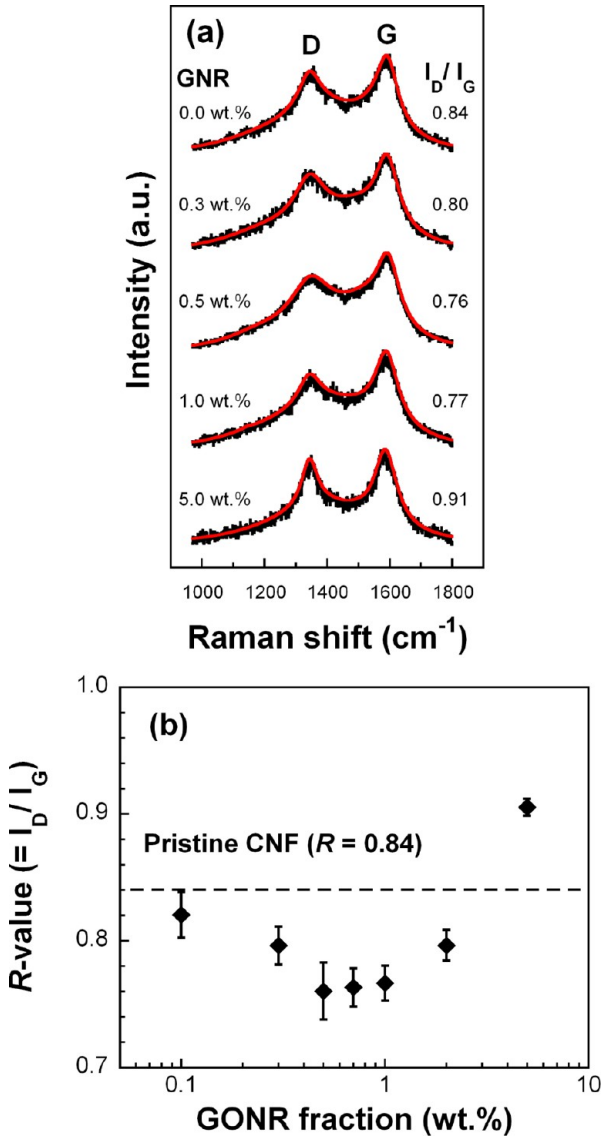

Figure 7. (a) Raman spectra and (b) *R*-value (= I_D/I_G) for the GNR/carbon composite nanofiber yarns with different GONR weight fractions.

than 0.5 wt % GONR fraction, the *R*-value increased (i.e., the crystallinity decreased). This supports the belief that the highly oriented GONRs in the nanofibers promote formation of ordered graphitic structures in the surroundings of the functional groups on the basal planes and edges of the GONRs during stabilization and carbonization. The oxygen-containing functional groups (e.g., hydroxyl end groups) can help to initiate the PAN cyclization and induced the aromatization during stabilization.[24−26] Analogously, the highly oriented GONRs in the PAN nanofibers would function as a promoter for the cyclization and aromatization, which would facilitate the further formation of ordered graphitic structures in the surroundings of the nanoribbon during stabilization. In addition, nanocarbons can act as nucleating and templating agents for the formation of a graphitic structure during carbonization.[27] More recently, Dzenis et al. reported that the incorporation of a small amount of double-walled carbon nanotubes into the electrospun PAN nanofibers significantly improved formation of the graphitic structure and crystal orientation of the carbonized composite fibers.[28]

The effects of the GONR content on the mechanical properties of the GNR/carbon composite nanofiber yarns were obtained from the stress−strain (*S*−*S*) curves (Figure S6, Supporting Information). The results are shown in Figure 8. The elongation was in the range of 0.4−0.7%. The tensile strength and the Young's modulus were significantly increased compared to those of the pristine PAN nanofiber yarns and PAN-based carbon nanofiber (CNF) yarns. The tensile strength showed a peak at the 0.5 wt % GONR fraction. The maximum strength of 382.4 MPa was 550% and 250% higher than those of the pristine PAN nanofiber yarns (69.7 MPa) and PAN-based CNF yarns (152.6 MPa), respectively. This value is also comparable to the GNR fibers spun from the liquid crystal phase solutions (378 MPa),[29] but lower than CNT fibers directly spun from CVD (~1.8 GPa assuming a density of 1 g cm^{-3}).[30] The GONR-fraction dependence on the tensile strength can be explained by the crystallinity (*R*-value, Figure 7b) of the carbonized composite nanofiber yarns. The Young's modulus, on the other hand, showed a peak at the 1 wt % GONR fraction. The maximum modulus of 53.6 GPa was 1620% and 180% higher than those of the PAN nanofiber yarns (3.3 GPa) and the PAN-based CNF yarns (30.3 GPa), respectively. The difference in the GONR fraction for the maximum values between the tensile strength and Young's modulus would depend on the internal structure of the

dx.doi.org/10.1021/am401161b | ACS Appl. Mater. Interfaces 2013, 5, 6225−6231

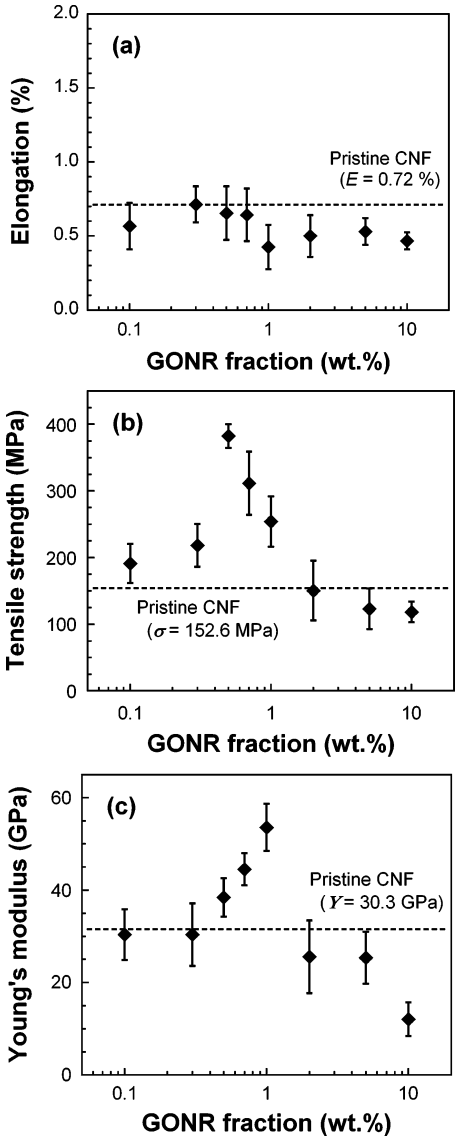

Figure 8. Effect of GONR content on the (a) elongation, (b) tensile strength, and (c) Young's modulus of the GNR/carbon composite nanofiber yarns.

composite nanofiber. For a more detailed discussion, a more precise characterization of the internal structure is required.

Figure 9 shows the additive effect of GONR on the electrical conductivity of the GNR/carbon composite nanofiber yarns. The electrical conductivity also showed a peak at the 0.5 wt % GONR fraction. This trend correlates well with the GONR-fraction dependence of the other properties (i.e., tensile strength and *R*-value). The maximum conductivity was 165.1 ± 4.3 S cm^{-1}. This value is larger than the maximum value of the reported electrospun carbon composite yarns (154 S cm^{-1} for the MWNT/carbon composite nanofiber yarns),[16] but lower than that of nanocarbon-based carbon fibers prepared by other spinning methods (285 S cm^{-1} for the GNR fibers from the liquid crystal phase solutions[29] and ~8000 S cm^{-1} for the single-walled CNT yarns from CVD[31]). Interestingly, this value was 220% higher than that of the PAN-based pristine CNF yarns (76.5 ± 2.0 S cm^{-1}) and about 300% higher than that of the monolayer GNR (53.6 S cm^{-1} for the annealed GNR (Figure S7, Supporting Information)). This also supported the hypothesis that the well-dispersed and highly oriented GONRs

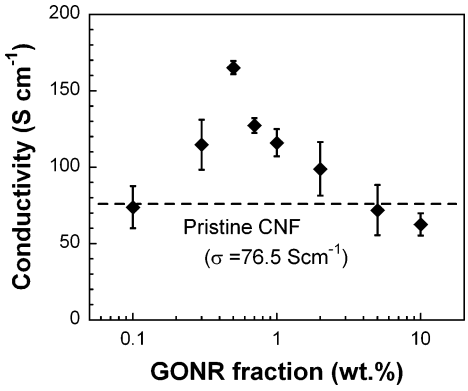

Figure 9. Effect of GONR content on the electrical conductivity of the GNR/carbon composite nanofiber yarns.

in the as-spun nanofibers enhanced the formation of the ordered graphitic structure during the stabilization and carbonization. At a less than 0.5 wt % GONR fraction, well-dispersed and highly oriented GONRs would enhance the formation of a continuous ordered graphitic structure along the fiber axis in the carbonized fibers. At a greater than 0.7 wt % GONR fraction, on the other hand, the agglomerates of GONRs would prevent formation of a continuous ordered graphitic structure in the fibers.

CONCLUSION

In conclusion, we demonstrated the fabrication of GNR/carbon composite nanofiber yarns by electrospinning of the GONR/PAN composites, followed by successive twisting and carbonization. The TEM analysis showed that the well-dispersed nanoribbons were highly oriented along the fiber axis in the electrospun fibers. This is due to the electrified thin liquid jet formed during electrospinning. A low weight fraction of the GONRs improved the mechanical properties of the composite nanofiber yarns. In addition, carbonization significantly enhanced the mechanical and electrical properties. Our characterizations supported the hypothesis that the GONRs contained in the nanofibers effectively functioned as not only the 1-D nanofiller but also the nanoplatelet promoter of stabilization and template agent for the carbonization. These results indicate that the GONR is a promising 1-D nanofiller for electrospun nanofiber-based composite materials. In particular, GONRs can potentially deliver synergistic simultaneous reinforcement and structural improvements. At present, we have not accomplished the optimization of the GNR/carbon composite nanofibers. It is expected that far better physical properties can be attained by optimization of spinning conditions (e.g., spinning solutions containing a higher content of well-dispersed GONRs or higher-aspect-ratio ones) and stabilization and carbonization conditions. The GNR/carbon composite nanofibers could be applied to reinforcements for lightweight composites and high-performance electrodes for fuel cells, fiber-shaped solar cells,[32] secondary batteries, and capacitors, including flexible and wearable electronic devices. In addition, a more detailed discussion of the formation mechanism of the graphitic structure in the nanofibers during stabilization and carbonization based on precise structural analyses (e.g., high-resolution TEM and microbeam X-ray scattering analysis) will be required. Further studies are now in progress, and the results will be reported.

dx.doi.org/10.1021/am401161b | ACS Appl. Mater. Interfaces 2013, 5, 6225−6231

■ ASSOCIATED CONTENT

Supporting Information

XRD patterns, XPS spectra, and Raman spectra of the starting MWNTs and the prepared GONRs; stress−strain curves for the as-spun GONR/PAN composite nanofiber yarns; FT-IR spectra of the stabilized GONR/PAN composite nanofiber yarns; TG curves of the stabilized GONR/PAN composite nanofiber yarns; stress−strain curves for the GNR/carbon composite nanofiber yarns; and *I*−*V* curves of the GNR device. This material is available free of charge via the Internet at http://pubs.acs.org.

■ AUTHOR INFORMATION

Corresponding Author

*E-mail: matsumoto.h.ac@m.titech.ac.jp (H.M.), tanioka.a.aa@m.titech.ac.jp (A.T.).

Notes

The authors declare no competing financial interest.

■ ACKNOWLEDGMENTS

The authors thank Professor H. Lipsanen, Department of Micro- and Nanosciences, Aalto University, Finland, for assistance with the FE-SEM observations, micro-Raman spectroscopy, and electrical conductivity measurements. This study was partly supported by the International Technology Center-Pacific (ITC-PAC), the U.S. Army Research Development and Engineering Command (RDECOM), and the U.S. Army Natic Soldier Center. S.I. gratefully acknowledges the Fellowship for Young Scientists (DC2, No. 239234) by the Japan Society for Promotion of Science, JSPS. The work at Rice University was funded by the AFOSR (FA9550-09-1-0581), AFOSR through the University Technology Corporation (09-S568-064-01-C1), and the AFOSR MURI (FA9550-12-1-00350).

■ REFERENCES

(1) Geim, A. K.; Novoselov, K. S. *Nat. Mater.* **2007**, *6*, 183−191.
(2) Lee, C.; Wei, X.; Kysar, J. W.; Hone, J. *Science* **2008**, *321*, 385−388.
(3) Balandin, A. A.; Ghosh, S.; Bao, W.; Calizo, I.; Teweldebrhan, D.; Miao, F.; Lau, C. N. *Nano Lett.* **2008**, *8*, 902−907.
(4) Kosynkin, D. V.; Higginbotham, A. L.; Sinitskii, A.; Lomeda, J. R.; Dimiev, A.; Price, B. K.; Tour, J. M. *Nature* **2009**, *458*, 872−876.
(5) Jiao, L.; Zhang, L.; Wang, X.; Diankov, G.; Dai, H. *Nature* **2009**, *458*, 877−880.
(6) Shimizu, T.; Haruyama, J.; Marcano, D. C.; Kosinkin, D. V.; Tour, J. M.; Hirose, K.; Suenaga, K. *Nat. Nanotechnol.* **2011**, *6*, 45−50.
(7) Kim, W. Y.; Kim, K. S. *Nat. Nanotechnol.* **2008**, *3*, 408−412.
(8) Terrones, M.; Botello-Méndez, A. R.; Campos-Delgado, J.; López-Urías, F.; Vega-Cantú, Y. I.; Rodríguez-Macías, F. J.; Elías, A. L.; Muñoz-Sandoval, E.; Cano-Márquez, A. G.; Charlier, J.-H.; Terrones, H. *Nano Today* **2010**, *5*, 351−372.
(9) Rafiee, M. A.; Lu, W.; Thomas, A. V.; Zandiatashbar, A.; Rafiee, J.; Tour, J. M.; Koratkar, N. A. *ACS Nano* **2010**, *4*, 7415−7420.
(10) Dimiev, A.; Lu, W.; Zeller, K.; Crowgey, B.; Kempel, L. C.; Tour, J. M. *ACS Appl. Mater. Interfaces* **2011**, *3*, 4657−4661.
(11) Bao, Q.; Zhang, H.; Yang, J.-X.; Wang, S.; Tang, D. Y.; Jose, R.; Ramakrishna, S.; Lim, C. T.; Loh, K. P. *Adv. Funct. Mater.* **2010**, *20*, 782−791.
(12) Farrar, D.; Ren, K.; Cheng, D.; Kim, S.; Moon, W.; Wilson, W. L.; West, J. E.; Yu, S. M. *Adv. Mater.* **2011**, *23*, 3954−3958.
(13) Doshi, J.; Reneker, D. H. *J. Electrost.* **1995**, *35*, 151−160.
(14) Reneker, D. H.; Chun, I. *Nanotechnology* **1996**, *7*, 216−223.
(15) Yarin, A. L.; Koombhongse, S.; Reneker, D. H. *J. Appl. Phys.* **2001**, *90*, 4836−4846.
(16) Imaizumi, S.; Matsumoto, H.; Konosu, Y.; Tsuboi, K.; Minagawa, M.; Tanioka, A.; Koziol, K.; Windle, A. *ACS Appl. Mater. Interfaces* **2011**, *3*, 469−475.
(17) Higginbotham, A. L.; Kosynkin, D. V.; Sinitskii, A.; Sun, Z.; Tour, J. M. *ACS Nano* **2010**, *4*, 2059−2069.
(18) Schniepp, H. C.; Li, J.-L.; McAllister, M. J.; Sai, H.; Herrera-Alonso, M.; Adamson, D. H.; Prud'homme, R. K.; Car, R.; Saville, D. A.; Aksay, I. A. *J. Phys. Chem. B* **2006**, *110*, 8535−8539.
(19) Nakashima, K.; Tsuboi, K.; Matsumoto, H.; Ishige, R.; Tokita, M.; Watanabe, J.; Tanioka, A. *Macromol. Rapid Commun.* **2010**, *31*, 1641−1645.
(20) Tsuboi, K.; Marcelletti, E.; Matsumoto, H.; Ashizawa, M.; Minagawa, M.; Furuya, H.; Akihiko Tanioka, A.; Abe, A. *Polym. J.* **2012**, *44*, 360−365.
(21) Hou, H.; Ge, J. J.; Zeng, J.; Li, Q.; Reneker, D. H.; Greiner, A.; Cheng, S. Z. D. *Chem. Mater.* **2005**, *17*, 967−973.
(22) Jawhari, T.; Roid, A.; Casado, J. *Carbon* **1995**, *33*, 1561−1565.
(23) Eklund, P. C.; Holden, J. M.; Jishi, R. A. *Carbon* **1995**, *33*, 959−972.
(24) Kim, J.; Kim, Y. C.; Ahn, W.; Kim, C. Y. *Polym. Eng. Sci.* **1993**, *33*, 1452−1457.
(25) Zhang, L.; Hsieh, Y.-L. *Nanotechnology* **2006**, *17*, 4416−4423.
(26) Zhou, Z.; Liu, K.; Lai, C.; Zhang, L.; Li, J.; Hou, H.; Reneker, D. H.; Hao, F. *Polymer* **2010**, *51*, 2360−2367.
(27) Min, B. G.; Chae, H. G.; Minus, M. L.; Kumar, S. In *Functional Composites of Carbon Nanotubes and Applications*; Lee, K.-P., Gopalan, A. I., Marquis, F. D. S., Eds.; Transworld Research Network: Kerlar, India, 2009; pp 51−55.
(28) Papkov, D.; Beese, A. M.; Goponenko, A.; Zou, Y.; Naraghi, M.; Espinosa, H. D.; Saha, B.; Schatz, G. C.; Moravsky, A.; Loutfy, R.; Nguyen, S. T.; Dzenis, Y. *ACS Nano* **2013**, *7*, 126−142.
(29) Xiang, C.; Behabtu, N.; Liu, Y.; Chae, H. G.; Young, C. C.; Genorio, B.; Tsentalovich, D. E.; Zhang, C.; Kosynkin, D. V.; Lomeda, J. R.; Hwang, C.-C.; Kumar, S.; Pasquali, M.; Tour, J. M. *ACS Nano* **2013**, *7*, 1628−1637.
(30) Boncel, S.; Sundaram, R. M.; Windle, A. H.; Koziol, K. K. *ACS Nano* **2011**, *5*, 9339−9344.
(31) Li, Y. L.; Kinloch, I. A.; Windle, A. H. *Science* **2004**, *304*, 276−278.
(32) Liu, D.; Zhao, M.; Li, Y.; Bian, Z.; Zhang, L.; Shang, Y.; Xia, X.; Zhang, S.; Yun, D.; Liu, Z.; Cao, A.; Huang, C. *ACS Nano* **2012**, *6*, 11027−11034.